

Möller and Bhabha scattering in the noncommutative standard model

P.K.Das,¹ N.G.Deshpande,² and G.Rajasekaran³

¹*Birla Institute of Technology and Science-Pilani,
Goa campus, NH-17B, Zuarinagar, Goa-403726, India*

²*Institute for Theoretical Science, University of Oregon, Eugene, OR 97403*

³*The Institute of Mathematical Sciences,
C.I.T Campus, Taramani, Chennai 600113, India*

(Dated: October 30, 2018)

Abstract

We study the Möller and Bhabha scattering in the noncommutative extension of the standard model(SM) using the Seiberg-Witten maps of this to first order of the noncommutative parameter $\theta_{\mu\nu}$. We look at the angular distribution $d\sigma/d\Omega$ to explore the noncommutativity of space-time at around $\Lambda_{NC} \sim \text{TeV}$ and find that the distribution deviates significantly from the one obtained from the commutative version of the standard model.

PACS: 11.10.Nx.

I. INTRODUCTION

Interest in the noncommutative field theory is old and it arose from the pioneering work by Snyder [1] and has been revived recently due to developments connected to string theories in which the noncommutativity of space-time is an important characteristic of D-brane dynamics at low energy limit[2, 3, 4, 5]. Although Douglas *et al.*[3] in their pioneering work have shown that noncommutative field theory is a well-defined quantum field theory, the question that remains whether string theory prediction and the noncommutative effect can be seen at the energy scale attainable in present or near future experiments instead of the 4-*d* Planck scale M_{pl} . A notable work by Witten *et al.*[7] suggests that one can see some stringy effects by lowering down the threshold value of commutativity to TeV, a scale which is not so far from present or future collider scale.

What is space-time noncommutativity? It means space and time no longer commute with each other. Now writing the space-time coordinates as operators (same as the position and momentum operator in quantum mechanics) we find

$$[\hat{X}_\mu, \hat{X}_\nu] = i\theta_{\mu\nu} = \frac{1}{\Lambda_{NC}^2} i c_{\mu\nu} \quad (1)$$

where $c_{\mu\nu}$ are antisymmetric constant parameters and Λ_{NC} is the scale at which space-time is no longer commutative. To study an ordinary field theory in such a noncommutative space-time one replaces all ordinary products among the field variables with Moyal-Weyl(MW) [8] \star products defined by

$$(f \star g)(x) = \exp\left(\frac{1}{2}\theta_{\mu\nu}\partial_{x^\mu}\partial_{y^\nu}\right) f(x)g(y)|_{y=x}. \quad (2)$$

Using this we can get the NCQED Lagrangian as

$$\mathcal{L} = \frac{1}{2}i(\bar{\psi} \star \gamma^\mu D_\mu \psi - (D_\mu \bar{\psi}) \star \gamma^\mu \psi) - m\bar{\psi} \star \psi - \frac{1}{4}F_{\mu\nu} \star F^{\mu\nu}, \quad (3)$$

which are invariant under the following transformations

$$\psi(x, \theta) \rightarrow \psi'(x, \theta) = U \star \psi(x, \theta), \quad (4)$$

$$A_\mu(x, \theta) \rightarrow A'_\mu(x, \theta) = U \star A_\mu(x, \theta) \star U^{-1} + \frac{i}{e}U \star \partial_\mu U^{-1}, \quad (5)$$

where $U = (e^{i\Lambda})_\star$. In the NCQED lagrangian (Eq.3) $D_\mu \psi = \partial_\mu \psi - ieA_\mu \star \psi$, $(D_\mu \bar{\psi}) = \partial_\mu \bar{\psi} + ie\bar{\psi} \star A_\mu$, $F_{\mu\nu} = \partial_\mu A_\nu - \partial_\nu A_\mu - ie(A_\mu \star A_\nu - A_\nu \star A_\mu)$.

The alternative one is the Seiberg-Witten(SW)[2, 3, 4, 6] approach in which both the gauge parameter Λ and the gauge field A^μ are expanded as

$$\Lambda_\alpha(x, \theta) = \alpha(x) + \theta^{\mu\nu} \Lambda_{\mu\nu}^{(1)}(x; \alpha) + \theta^{\mu\nu} \theta^{\eta\sigma} \Lambda_{\mu\nu\eta\sigma}^{(2)}(x; \alpha) + \dots \quad (6)$$

$$A_\rho(x, \theta) = A_\rho(x) + \theta^{\mu\nu} A_{\mu\nu\rho}^{(1)}(x) + \theta^{\mu\nu} \theta^{\eta\sigma} A_{\mu\nu\eta\sigma\rho}^{(2)}(x) + \dots \quad (7)$$

and when the field theory is expanded in terms of this power series (6) one end up with an infinite tower of higher dimensional operators which renders the theory nonrenormalizable. However, the advantage is that this construction can be applied to any gauge theory with arbitrary matter representation. In the MW approach the group closure property was found to hold only for $U(N)$ gauge theories with matter content in the fundamental or adjoint representations. Using the SW-map, Calmet *et al.*[9] first constructed a model with non-commutative gauge invariance which was close to the usual Standard Model and is known as the *minimal* NCSM(mNCSM) and they listed several Feynman rules. Many phenomenological studies [10] have been made to unravel several interesting features of this mNCSM. Hewett *et al.* explored several processes e.g. $e^+e^- \rightarrow e^+e^-$ (Bhabha), $e^-e^- \rightarrow e^-e^-$ (Möller), $e^- \gamma \rightarrow e^- \gamma$, $e^+e^- \rightarrow \gamma\gamma$ (pair annihilation), $\gamma\gamma \rightarrow e^+e^-$ and $\gamma\gamma \rightarrow \gamma\gamma$ in context of NCQED. They found that the differential cross-section for Bhabha scattering(a s-channel process) is dependent on the space-time NC parameters θ_{0i} , ($i = 1, 2, 3$), whereas in Möller scattering(a t and u-channel dominated process) the sensitivities are on θ_{12} and θ_{13} , if the beam is in the 1-direction. However, their analyses were only in the context of NCQED, not in full mNCSM, i.e. they didn't consider the impact of the neutral Z boson exchange in Bhabha and Möller scattering. Here we consider the impact of both Z and photon exchange in our analysis of the above two processes in the NC framework and will see the modification in the angular distribution of the differential cross-section which arise both from the polar(θ^*) and the azimuthal angular(ϕ) dependences. Note that in the earlier analyses only the ϕ distribution of the cross-section was studied, whereas in this work we study also the polar distribution. Since we have the Z mediated diagrams, the interference term between the photon and Z mediated Feynman diagrams, do have some impact on such distribution, which in other words is nothing but a measure of direct CP-asymmetry. Now in a generic NCQED the triple photon arises to order θ , which however is absent in this minimal mNCSM. Another formulation of the NCSM came in forefront through the pioneering work by Melic *et al.*[11] where such a triple neutral gauge boson coupling [12] appears naturally

in the gauge sector. We will call this the non-minimal version of NCSM or simply NCSM. In the present work we will confine ourselves within this non-minimal version of the NCSM and use the Feynman rules for interactions given in Melic *et al.*[11].

II. MÖLLER SCATTERING IN THE NCSM

The Möller scattering $e^-(p_1)e^-(p_2) \rightarrow e^-(p_3)e^-(p_4)$ in the NCSM proceeds via the t and u channel exchange of γ and Z boson just like the usual SM(which is a commutative one and is being described as CSM). The corresponding Feynman diagrams are shown in Fig. 1

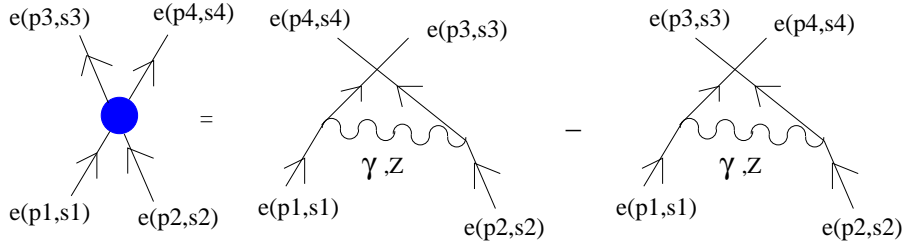


FIG. 1: Feynman diagrams for the Möller scattering.

The scattering amplitude to order θ , for the photon mediated diagrams can be written as

$$\begin{aligned} \mathcal{A}_M^\gamma &= e^2 \left[\left(1 - \frac{i}{2}p_4\theta p_2 + \frac{i}{2}p_3\theta p_1\right) \bar{u}(p_3, s_3) \gamma^\mu u(p_1, s_1) \bar{u}(p_4, s_4) \gamma_\mu u(p_2, s_2) \left(\frac{i}{t}\right) \right] \\ &\quad - e^2 \left[\left(1 - \frac{i}{2}p_3\theta p_2 + \frac{i}{2}p_4\theta p_1\right) \bar{u}(p_4, s_4) \gamma^\mu u(p_1, s_1) \bar{u}(p_3, s_3) \gamma_\mu u(p_2, s_2) \left(\frac{i}{u}\right) \right] \\ &= \mathcal{A}_{1M}^\gamma - \mathcal{A}_{2M}^\gamma, \end{aligned} \quad (8)$$

and for the Z boson mediated diagrams as

$$\begin{aligned} \mathcal{A}_M^Z &= \frac{e^2}{x_W^2} \left[\left(1 - \frac{i}{2}p_4\theta p_2 + \frac{i}{2}p_3\theta p_1\right) \bar{u}(p_3, s_3) \gamma^\mu \Gamma_A^- u(p_1, s_1) \bar{u}(p_4, s_4) \gamma_\mu \Gamma_A^- u(p_2, s_2) \left(\frac{i}{t - m_Z^2}\right) \right] \\ &\quad - \frac{e^2}{x_W^2} \left[\left(1 - \frac{i}{2}p_3\theta p_2 + \frac{i}{2}p_4\theta p_1\right) \bar{u}(p_4, s_4) \gamma^\mu \Gamma_A^- u(p_1, s_1) \bar{u}(p_3, s_3) \gamma_\mu \Gamma_A^- u(p_2, s_2) \left(\frac{i}{u - m_Z^2}\right) \right] \\ &= \mathcal{A}_{1M}^Z - \mathcal{A}_{2M}^Z \end{aligned} \quad (9)$$

where $p_1\theta p_2 = p_1^\mu \theta_{\mu\nu} p_2^\nu$, $p_1 + p_2 = p_3 + p_4$, $t = (p_1 - p_3)^2$, $u = (p_1 - p_4)^2$, and $s = (p_1 + p_2)^2$. Also $x_W = \sin 2\theta_W$ (θ_W , the Weinberg angle), $\Gamma_A^\pm = c_V^e \pm c_A^e \gamma_5$ with $c_V^e = T_3^e - 2Q_e \sin^2 \theta_W$ and $c_A^e = T_3^e$.

The spin-averaged and summed squared-amplitude is given by

$$\begin{aligned} |\overline{\mathcal{A}}_M|^2 &= |\overline{\mathcal{A}}_{1M}^\gamma|^2 + |\overline{\mathcal{A}}_{2M}^\gamma|^2 + |\overline{\mathcal{A}}_{1M}^Z|^2 + |\overline{\mathcal{A}}_{2M}^Z|^2 - 2\overline{\text{Re}}(\overline{\mathcal{A}}_{1M}^\gamma \overline{\mathcal{A}}_{2M}^{\gamma*}) - 2\overline{\text{Re}}(\overline{\mathcal{A}}_{1M}^Z \overline{\mathcal{A}}_{2M}^{Z*}) + 2\overline{\text{Re}}(\overline{\mathcal{A}}_{1M}^\gamma \overline{\mathcal{A}}_{1M}^{Z*}) \\ &\quad - 2\overline{\text{Re}}(\overline{\mathcal{A}}_{1M}^\gamma \overline{\mathcal{A}}_{2M}^{Z*}) - 2\overline{\text{Re}}(\overline{\mathcal{A}}_{2M}^\gamma \overline{\mathcal{A}}_{1M}^{Z*}) + 2\overline{\text{Re}}(\overline{\mathcal{A}}_{2M}^\gamma \overline{\mathcal{A}}_{2M}^{Z*}) = \frac{1}{4} \sum_{\text{spins}} |\mathcal{A}_M^\gamma + \mathcal{A}_M^Z|^2. \end{aligned} \quad (10)$$

Several terms in the squared-amplitude are given in Appendix B.

III. BHABHA SCATTERING IN THE NC STANDARD MODEL

Next the Bhabha scattering $e^-(p_1)e^+(p_2) \rightarrow e^-(p_3)e^+(p_4)$. As in the usual SM, the Bhabha scattering in the NCSM proceeds via the s and t channel exchange of γ and Z bosons. The respective Feynman diagrams are shown in Fig. 2

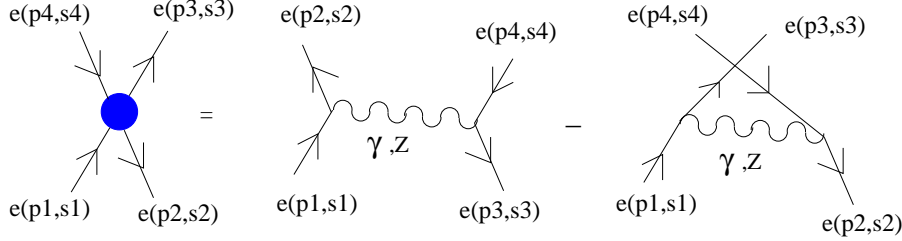


FIG. 2: Feynman diagrams for the Bhabha scattering.

The scattering amplitude to order θ , for the photon mediated diagram can be written as

$$\begin{aligned} \mathcal{A}_B^\gamma &= e^2 \left[\left(1 + \frac{i}{2}p_2\theta p_1 + \frac{i}{2}p_4\theta p_3\right) \bar{v}(p_2, s_2) \gamma^\mu u(p_1, s_1) \bar{u}(p_3, s_3) \gamma_\mu v(p_4, s_4) \left(\frac{i}{s}\right) \right] \\ &\quad - e^2 \left[\left(1 - \frac{i}{2}p_3\theta p_1 - \frac{i}{2}p_4\theta p_2\right) \bar{u}(p_3, s_3) \gamma^\mu u(p_1, s_1) \bar{v}(p_2, s_2) \gamma_\mu v(p_4, s_4) \left(\frac{i}{t}\right) \right] \\ &= \mathcal{A}_{1B}^\gamma - \mathcal{A}_{2B}^\gamma, \end{aligned} \quad (11)$$

and for the Z mediated diagram as

$$\begin{aligned} \mathcal{A}_B^Z &= \frac{e^2}{x_W^2} \left[\left(1 + \frac{i}{2}p_2\theta p_1 + \frac{i}{2}p_4\theta p_3\right) \bar{v}(p_2, s_2) \gamma^\mu \Gamma_A^- u(p_1, s_1) \bar{u}(p_3, s_3) \gamma_\mu \Gamma_A^- v(p_4, s_4) \left(\frac{i}{s - m_Z^2}\right) \right] \\ &\quad - \frac{e^2}{x_W^2} \left[\left(1 - \frac{i}{2}p_3\theta p_1 - \frac{i}{2}p_4\theta p_2\right) \bar{u}(p_3, s_3) \gamma^\mu \Gamma_A^- v(p_1, s_1) \bar{v}(p_2, s_2) \gamma_\mu \Gamma_A^- v(p_4, s_4) \left(\frac{i}{t - m_Z^2}\right) \right] \\ &= \mathcal{A}_{1B}^Z - \mathcal{A}_{2B}^Z. \end{aligned} \quad (12)$$

The spin-averaged and summed squared-amplitude can be written as

$$\begin{aligned} \overline{|\mathcal{A}_B|^2} &= \overline{|\mathcal{A}_{1B}^\gamma|^2} + \overline{|\mathcal{A}_{2B}^\gamma|^2} + \overline{|\mathcal{A}_{1B}^Z|^2} + \overline{|\mathcal{A}_{2B}^Z|^2} - 2\overline{Re(\mathcal{A}_{1B}^\gamma \mathcal{A}_{2B}^{\gamma*})} - 2\overline{Re(\mathcal{A}_{1B}^Z \mathcal{A}_{2B}^{Z*})} + 2\overline{Re(\mathcal{A}_{1B}^\gamma \mathcal{A}_{1B}^{Z*})} \\ &\quad - 2\overline{Re(\mathcal{A}_{1B}^\gamma \mathcal{A}_{2B}^{Z*})} - 2\overline{Re(\mathcal{A}_{2B}^\gamma \mathcal{A}_{1B}^{Z*})} + 2\overline{Re(\mathcal{A}_{2B}^\gamma \mathcal{A}_{2B}^{Z*})} = \frac{1}{4} \sum_{spins} |\mathcal{A}_B^\gamma + \mathcal{A}_B^Z|^2. \end{aligned} \quad (13)$$

Several terms in the squared-amplitude are given in Appendix C.

The differential cross-section of a $2 \rightarrow 2$ scattering (Möller or Bhabha) reads as

$$\frac{d\sigma}{d\Omega} = \frac{1}{64\pi^2 s^2} \beta \overline{|\mathcal{A}|^2} = \frac{1}{64\pi^2 s} \overline{|\mathcal{A}|^2} \quad (14)$$

where $\beta = s(1 - 4m^2/s)^{1/2} \simeq s$ (since $\sqrt{s} \gg 2m$) and $d\Omega = d\cos\theta^* d\phi$. The amplitude square $|\mathcal{A}|^2$ corresponds to $|\mathcal{A}_M|^2$ for Möller scattering and $|\mathcal{A}_B|^2$ for Bhabha scattering.

IV. NUMERICAL ANALYSIS

After obtaining the angular distributions of the differential cross-section in the presence of space-time noncommutativity, we then analyze the distributions. In our analysis, we set the machine energy at $\sqrt{s}(= E_{com}) = 1500$ GeV.

A. Angular distribution of the Möller scattering in the NCSM

In Figs. 3(a,b) we have shown the angular distribution $\frac{d\sigma}{d\Omega}$ as a function of the azimuthal angle ϕ with θ^* (polar angle) being fixed at $\pi/4$ and $3\pi/4$, respectively. In the usual SM, the azimuthal distribution is supposed to be flat and the lowest horizontal curve in Figs. 3a and 3b, corresponds to that. Note the differences between figures for different θ^* and among different curves for a given θ^* . In Fig. 3a(or 3b), the topmost curve corresponds to $\Lambda_{NC} = 800$ GeV and this differs maximally from the CSM flat curve. The 2nd and 3rd curves (moving from the top) stands for $\Lambda_{NC} = 1000$ and 1200 GeV and they still lie above the flat curve. This is essentially due to the factor $\cos\phi + \sin\phi$ whose origin is in the

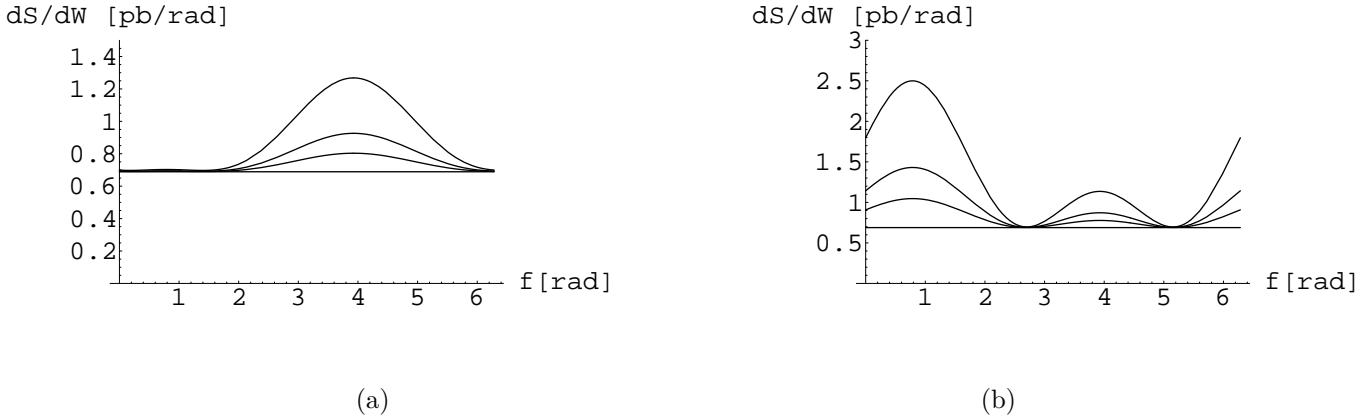


FIG. 3. The $\frac{d\sigma}{d\Omega}$ (pb/radian) distribution (for fixed θ^*) as a function of the ϕ (in radian) for Möller scattering. θ^* is chosen as $\pi/4$ and $3\pi/4$, respectively. The c.o.m energy (E_{com}) is fixed at $\sqrt{s} = 1500$ GeV. The lowest horizontal curve is due to the commutative SM. Note that $\frac{d\sigma}{d\Omega}$ and ϕ appear, respectively, as ds/dW and f in these and later figures.

noncommutativity of space-time and which is simply the identity in the CSM. Note that the deviation from the CSM prediction is maximal in a wide region (from small to large values) of ϕ (see Figs. 3a and 3b). In Figs. 3(c)-3(f), $d\sigma/d\Omega$ is plotted as a function of $\cos\theta^*$ with ϕ being fixed at $= 0, \pi/2, \pi$ and $3\pi/2$, respectively. As before, the lowest curve in each of these figures is due to the CSM, whereas the topmost, next to the top and next to that (second from the lowest one) respectively stands for $\Lambda_{NC} = 800, 1000$ and 1200 . Differences between these figures are worthwhile to note. Obviously the distribution is asymmetric around $\cos\theta^* = 0$ (which means $\theta^* = \pi/2$) axis. Such an asymmetry which is non-vanishing in the CSM due to the γ and Z amplitude interference terms (the lowest curve corresponds to that), increases with the decrease of Λ_{NC} . For example the asymmetry corresponding to $\Lambda_{NC} = 800$ GeV is greater than that obtained at $\Lambda_{NC} = 1200$. So the noncommutative geometry does indeed have an impact on the $\cos\theta^*$ distribution and thus on the direct CP asymmetry A_{CP} in case of Möller scattering. Note that the earlier authors [10] while studying the Möller scattering, did not study such an asymmetry, which we did and is one of our main result in this work.

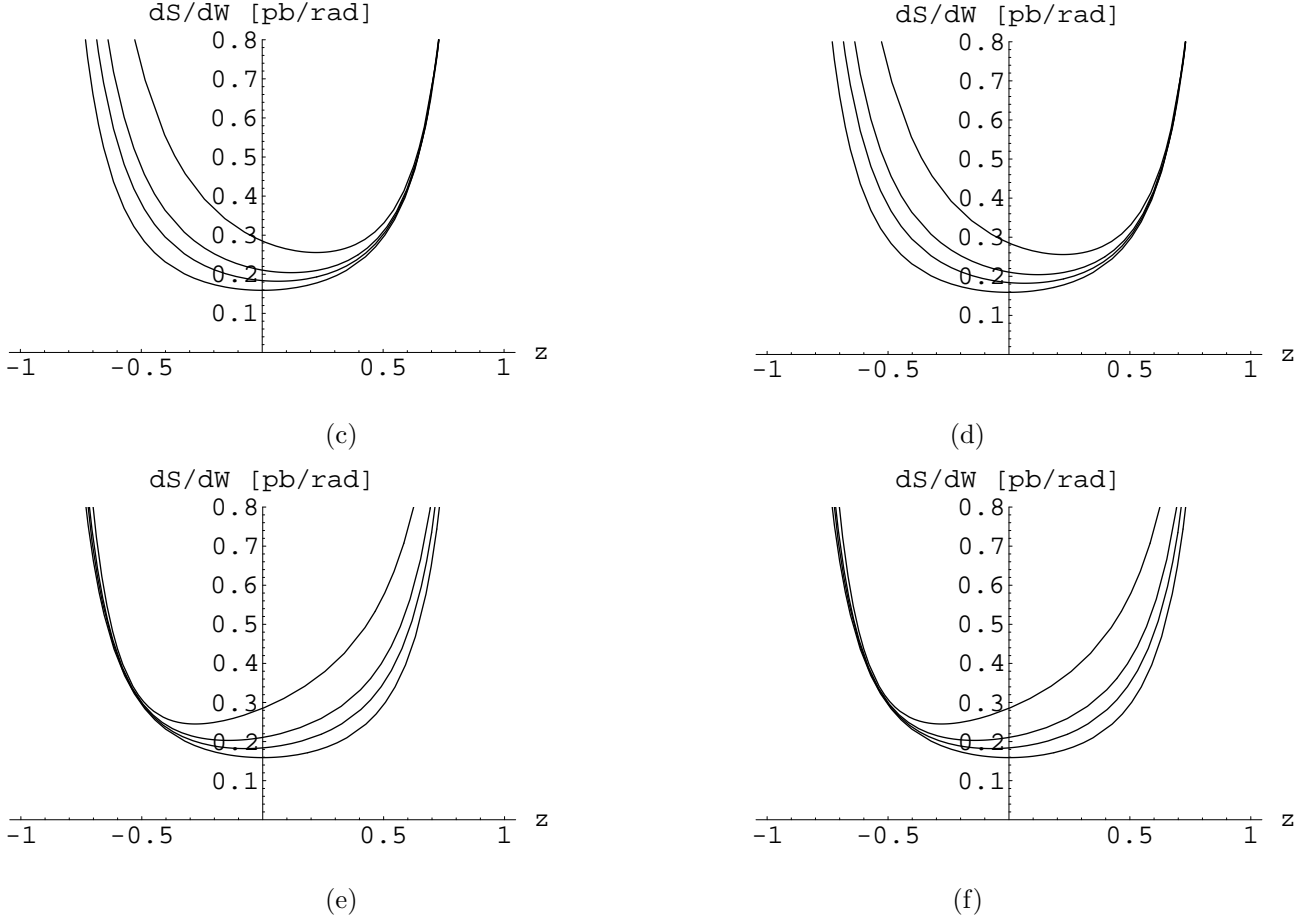
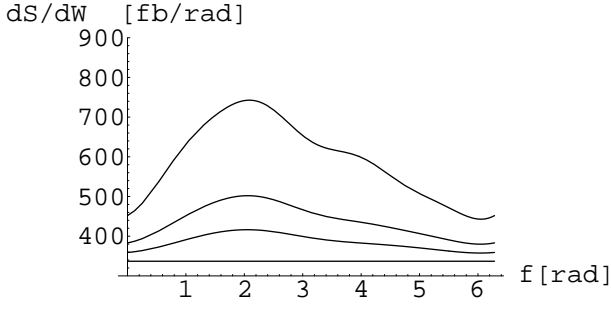


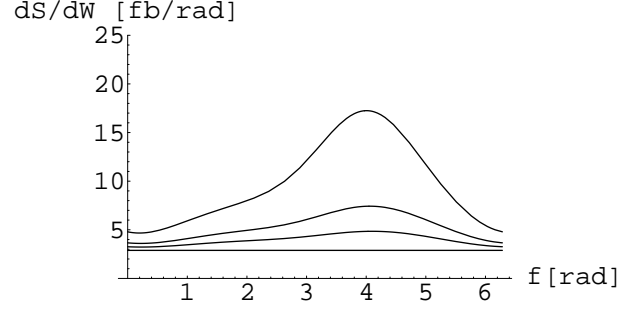
FIG. 3. The polar distribution $\frac{d\sigma}{d\Omega}$ (pb/radian) as a function of the $\cos\theta^*$ (in radian) for the Möller scattering. The azimuthal angle ϕ is kept fixed at $0, \pi/2, 3\pi$ and $3\pi/2$. The lowest curve in each of these figures is due to the commutative SM. Note that $\cos\theta^*$ appear as z in these and later figures.

B. Angular distribution of the Bhabha scattering in the NCSM

We next turn our attention to the Bhabha scattering and examine the impact of space-time noncommutativity on the angular distribution. In Figs. 3g and 3h, we have plotted the distribution $\frac{d\sigma}{d\Omega}$ as a function of the azimuthal angle ϕ for fixed θ^* and it is $\pi/4$ for Fig. 3g and $3\pi/4$ for Fig. 3h, respectively. The azimuthal distribution in the usual SM(CSM) is completely flat and in each figure the lowest flat curve resembles to that. Note the differences



(g)



(h)

FIG. 3. The $\frac{d\sigma}{d\Omega}$ (fb/radian) distribution (for fixed θ^*) as a function of the ϕ (in radian) for Bhabha scattering. θ^* is fixed at $\pi/4$ and $3\pi/4$. We choose the c.o.m energy(E_{com}) equal to $\sqrt{s} = 1500$ GeV. The lowest horizontal curve is the commutative SM result.

between figures for different θ^* (i.e. Figs. 3g and 3h) and among different curves for a given θ^* (i.e. in Fig. 3g or 3h). In Fig. 3g(or 3h), the topmost curve corresponds to $\Lambda_{NC} = 800$ GeV and the 2nd and 3rd one (starting from the topmost one) stands for $\Lambda_{NC} = 1000$ GeV and 1200 GeV, respectively. Note that the topmost curve(in either Fig.) differs maximally from the CSM flat curve and the other two still lie above the flat curve and this is due to the same ϕ dependent factor as discussed in earlier section. Also note that the deviation from the CSM flat curve is maximal in a wide region (from small to large values) of ϕ (see Figs. 3g and 3h).

In Figs. 3(i)-3(l) we have plotted $d\sigma/d\Omega$ as a function of $\cos\theta^*$ for fixed ϕ . ϕ is chosen as $0, \pi/2, \pi$ and $3\pi/2$, respectively. The lowest curve in each of these figures is due to the CSM, whereas the topmost, next to the top and next to that (second from the lowest one) respectively stands for $\Lambda_{NC} = 800, 1000$ and 1200. Obviously the distribution which is asymmetric around $\cos\theta^* = 0$ (i.e. $\theta^* = \pi/2$) axis, as is expected within the CSM due to the γ and Z interference terms, increases with the decrease of Λ_{NC} . The lowest curve(in each of these figures) corresponds to that due to the CSM. Note the change in asymmetry prediction with the change in fixed ϕ value which is minimum for $\phi = 0$ and maximum for $\phi = \pi/2$. Also to note that the asymmetry at $\Lambda_{NC} = 800$ GeV is greater than that obtained at $\Lambda_{NC} = 1200$ in a given curve. So the noncommutative geometry does indeed have an

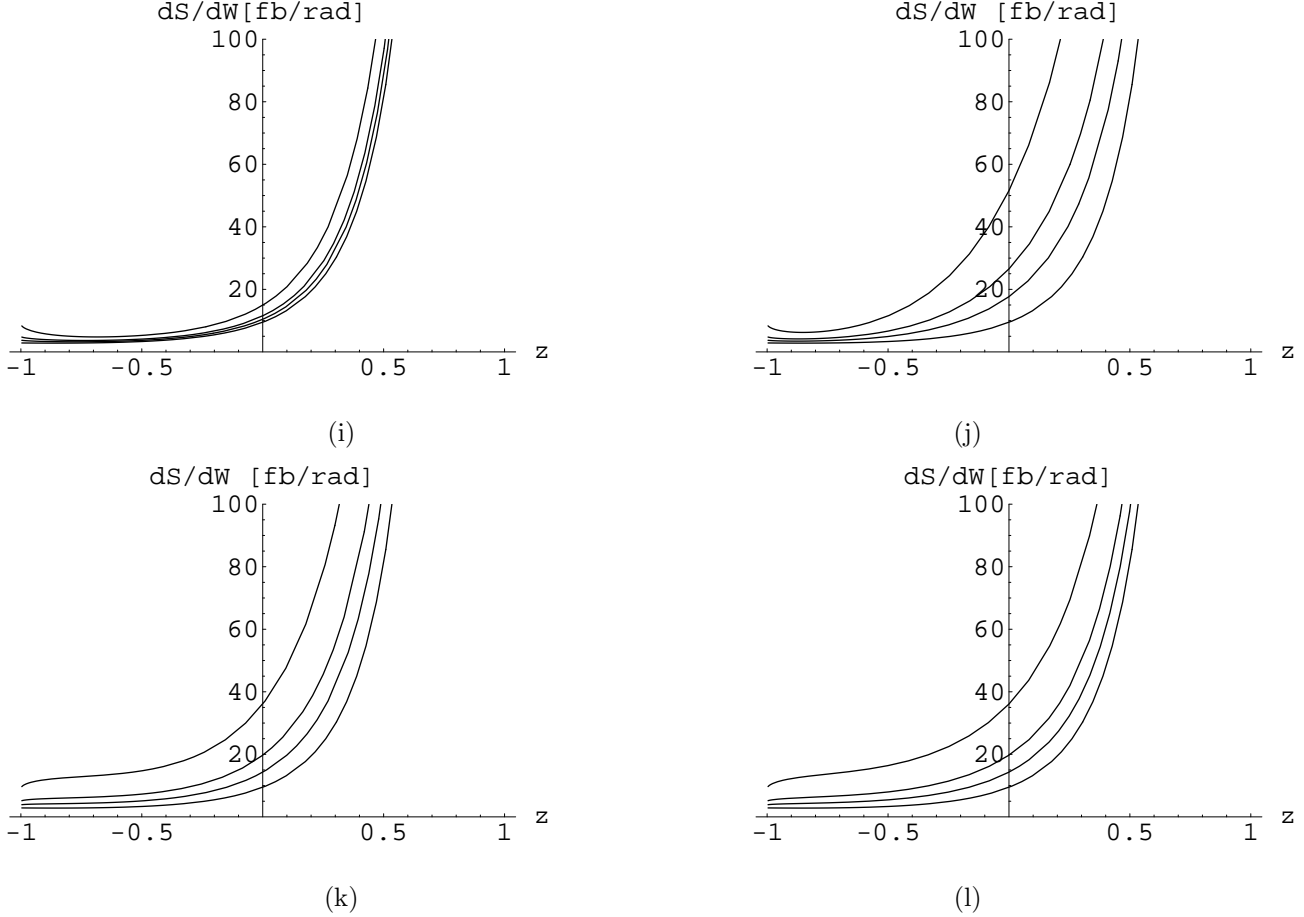


FIG. 3. The polar distribution $\frac{d\sigma}{d\Omega}$ (fb/radian) as a function of the $\cos\theta^*$ (in radian) for the Bhabha scattering. The azimuthal angle ϕ is kept fixed at $0, \pi/2, 3\pi$ and $3\pi/2$, respectively. The lowest curve in each of these figures is due to the commutative SM.

impact on the $\cos\theta^*$ distribution and thus on A_{CP} in case of Bhabha scattering. Note that the earlier authors [10] did not include Z -mediated diagram while studying the Bhabha scattering and thus didn't pay attention on such asymmetry plot. We consider the Z mediated amplitude and the impact of the space-time noncommutativity on such an asymmetry plot and is one of the main result of the present work.

V. CONCLUSION

The idea that around the TeV scale the space and time coordinates no longer remains commutative in nature (and becomes non-commutative) is explored here by investigating its impact on the two fundamental processes, the Möller and Bhabha scattering. In addition to the photon exchange, we considered here also the Z boson exchange, which leads to

substantial amount of modification of earlier works(in which Z -exchange was not considered). From the azimuthal distribution $d\sigma/d\Omega$ for a fixed θ^* we see that for certain θ^* ($\pi/4$ and $3\pi/4$) the distribution differs significantly from the one expected from the commutative version of the SM. At around $\Lambda_{NC} \sim 1500$ (noting that $E_{cm} = 1500$ GeV in this analysis) the NC effect smeared out, what remains is the one(the flat curve) as expected within the CSM. With the lowering of Λ_{NC} , say for example from 1200 GeV to 500 GeV, the NC effect gets enhanced. Besides the azimuthal distribution, we also obtain the polar distribution $d\sigma/d\Omega$ for a fixed ϕ and hence the direct CP-asymmetry. We observed that such distribution do really depend on θ^* and have an asymmetry which simply got an enhancement for certain ϕ value (e.g. $\phi = \pi/2$ and $3\pi/2$). Such a result is completely new. Combining the azimuthal and polar distribution, we found that for the c.o.m energy $E_{cm} = 1500$ GeV, the noncommutative effect do manifests itself at around $\Lambda_{NC} \sim 800$ to 1200 GeV and differs significantly from the curve (the lowest horizontal curve in each plot) obtained from the commutative version of the SM.

Acknowledgments

P. K. Das would like to thank Prof T.R.Govindrajan of IMSc,Chennai for useful discussions during his stay at IMSc. The work of N.G.Deshpande is supported by the US DOE under Grant No. DE-FG02-96ER40969.

APPENDIX A: FEYNMAN RULES TO ORDER $\mathcal{O}(\theta)$

We follow the Reference [11] for the Feynman rule for several interactions, propagators. The Feynman rule for the $e(p_{in}) - e(p_{out}) - \gamma(k)$ vertex to $O(\theta)$ is

$$\begin{aligned} & ieQ_f \left[\gamma_\mu - \frac{i}{2} k^\nu (\theta_{\mu\nu\rho} p_{in}^\rho - \theta_{\mu\nu} m_f) \right] \\ & = ieQ_f \gamma_\mu + \frac{1}{2} eQ_f [(p_{out}\theta p_{in})\gamma_\mu - (p_{put}\theta)_\mu(\not{p}_{in} - m_f) - (\not{p}_{out} - m_f)(\theta p_{in})_\mu], \end{aligned}$$

and for the vertex $e(p_{in}) - e(p_{out}) - Z(k)$ is

$$\frac{e}{\sin 2\theta_W} [i\gamma_\mu \Gamma_A^-] + \frac{e}{2\sin 2\theta_W} [(p_{out}\theta p_{in})\gamma_\mu \Gamma_A^- - (p_{put}\theta)_\mu \Gamma_A^+(\not{p}_{in} - m_f) - (\not{p}_{out} - m_f) \Gamma_A^-(\theta p_{in})_\mu].$$

Here $\theta_{\mu\nu\rho} = \theta_{\mu\nu}\gamma_\rho + \theta_{\nu\rho}\gamma_\mu + \theta_{\rho\mu}\gamma_\nu$, $\Gamma_A^\pm = (c_V^e \pm c_A^e \gamma_5)$ and $Q_f = \mp 1$ for e^\mp .

Also $p_{out}\theta p_{in} = p_{out}^\mu \theta_{\mu\nu} p_{in}^\nu = -p_{in}\theta p_{out}$. The momentum conservation reads as $p_{in} + k = p_{out}$.

APPENDIX B: SQUARED AMPLITUDE OF THE MÖLLER ($e^-(p_1)e^-(p_2) \rightarrow e^-(p_3)e^-(p_4)$) **SCATTERING**

Here we explicitly present several squared-amplitude terms of Eq.(10). Defining p_1 , p_2 , p_3 and p_4 to be the momenta of the of the initial and final state electrons, the terms in the squared matrix element are given by

$$\begin{aligned}
|\overline{\mathcal{A}_{1M}^\gamma}|^2 &= \frac{e^4}{4t^2} \left(1 + \frac{1}{4}A^2\right) Tr[\not{p}_1\gamma_\nu\not{p}_3\gamma_\mu] \times Tr[\not{p}_2\gamma^\nu\not{p}_4\gamma^\mu], \\
|\overline{\mathcal{A}_{2M}^\gamma}|^2 &= \frac{e^4}{4u^2} \left(1 + \frac{1}{4}B^2\right) Tr[\not{p}_1\gamma_\nu\not{p}_3\gamma_\mu] \times Tr[\not{p}_2\gamma^\nu\not{p}_4\gamma^\mu], \\
|\overline{\mathcal{A}_{1M}^Z}|^2 &= \frac{e^4}{4x_W^4(t-m_Z^2)^2} \left(1 + \frac{1}{4}A^2\right) Tr[\not{p}_1\gamma_\nu\Gamma_A^-\not{p}_3\gamma_\mu\Gamma_A^-] \times Tr[\not{p}_2\gamma^\nu\Gamma_A^-\not{p}_4\gamma^\mu\Gamma_A^-], \\
|\overline{\mathcal{A}_{2M}^Z}|^2 &= \frac{e^4}{4x_W^4(u-m_Z^2)^2} \left(1 + \frac{1}{4}B^2\right) Tr[\not{p}_1\gamma_\nu\Gamma_A^-\not{p}_3\gamma_\mu\Gamma_A^-] \times Tr[\not{p}_2\gamma^\nu\Gamma_A^-\not{p}_4\gamma^\mu\Gamma_A^-], \\
-2\overline{Re(\mathcal{A}_{1M}^\gamma\mathcal{A}_{2M}^{\gamma*})} &= -\frac{e^4}{2ut} Re \left[\left(1 + \frac{i}{2}A\right)\left(1 - \frac{i}{2}B\right) Tr[\not{p}_1\gamma_\nu\not{p}_4\gamma_\mu\not{p}_2\gamma^\nu\not{p}_3\gamma^\mu] \right], \\
-2\overline{Re(\mathcal{A}_{1M}^Z\mathcal{A}_{2M}^{Z*})} &= -\frac{e^4}{2x_W^4(u-m_Z^2)(t-m_Z^2)} Re \left[\left(1 + \frac{i}{2}A\right)\left(1 - \frac{i}{2}B\right) Tr[\not{p}_1\gamma_\nu\Gamma_A^-\not{p}_4\gamma_\mu\Gamma_A^-\not{p}_2\gamma^\nu\Gamma_A^-\not{p}_3\gamma^\mu\Gamma_A^-] \right], \\
+2\overline{Re(\mathcal{A}_{1M}^\gamma\mathcal{A}_{1M}^{Z*})} &= \frac{e^4}{2x_W^2t(t-m_Z^2)} Re \left[\left(1 + \frac{1}{4}A^2\right) Tr[\not{p}_1\gamma_\nu\Gamma_A^-\not{p}_3\gamma_\mu] Tr[\not{p}_2\gamma^\nu\Gamma_A^-\not{p}_4\gamma^\mu] \right], \\
-2\overline{Re(\mathcal{A}_{1M}^\gamma\mathcal{A}_{2M}^{Z*})} &= -\frac{e^4}{2x_W^2t(u-m_Z^2)} Re \left[\left(1 + \frac{i}{2}A\right)\left(1 - \frac{i}{2}B\right) Tr[\not{p}_1\gamma_\nu\Gamma_A^-\not{p}_4\gamma_\mu\not{p}_2\gamma^\nu\Gamma_A^-\not{p}_3\gamma^\mu] \right], \\
-2\overline{Re(\mathcal{A}_{2M}^\gamma\mathcal{A}_{1M}^{Z*})} &= -\frac{e^4}{2x_W^2u(t-m_Z^2)} Re \left[\left(1 + \frac{i}{2}A\right)\left(1 - \frac{i}{2}B\right) Tr[\not{p}_1\gamma_\nu\Gamma_A^-\not{p}_3\gamma_\mu\not{p}_2\gamma^\nu\Gamma_A^-\not{p}_4\gamma^\mu] \right], \\
+2\overline{Re(\mathcal{A}_{2M}^\gamma\mathcal{A}_{2M}^{Z*})} &= \frac{e^4}{2x_W^2u(u-m_Z^2)} Re \left[\left(1 + \frac{1}{4}B^2\right) Tr[\not{p}_1\gamma_\nu\Gamma_A^-\not{p}_4\gamma_\mu] Tr[\not{p}_2\gamma^\nu\Gamma_A^-\not{p}_3\gamma^\mu] \right],
\end{aligned} \tag{B1}$$

where $A = (p_3\theta p_1 - p_4\theta p_2)$ and $B = (p_4\theta p_1 - p_3\theta p_2)$.

In the c.o.m frame of $e^-(p_1)$ and $e^-(p_2)$ collision, the following prescription for the 4-momenta are used:

$$\begin{aligned}
p_1 &= \left(\frac{\sqrt{s}}{2}, 0, 0, \frac{\sqrt{s}}{2}\right) = (E_1, \vec{P}_1), \\
p_2 &= \left(\frac{\sqrt{s}}{2}, 0, 0, -\frac{\sqrt{s}}{2}\right) = (E_2, \vec{P}_2), \\
p_3 &= \left(\frac{\sqrt{s}}{2}, \frac{\sqrt{s}}{2}\sin\theta^*\cos\phi, \frac{\sqrt{s}}{2}\sin\theta^*\sin\phi, \frac{\sqrt{s}}{2}\cos\theta^*\right) = (E_3, \vec{P}_3), \\
p_4 &= \left(\frac{\sqrt{s}}{2}, -\frac{\sqrt{s}}{2}\sin\theta^*\cos\phi, -\frac{\sqrt{s}}{2}\sin\theta^*\sin\phi, -\frac{\sqrt{s}}{2}\cos\theta^*\right) = (E_4, \vec{P}_4),
\end{aligned} \tag{B2}$$

where θ^* is the scattering angle made by the 3-momentum vector p_3 of $e^-(p_3)$ with the z axis and ϕ is the azimuthal angle. In above $m = m_e \simeq 0$. Note that $\vec{P}_1 = |P_1|\hat{z}$, $\vec{P}_2 = -|P_2|\hat{z}$ and $\vec{P}_1 + \vec{P}_2 = 0 = \vec{P}_3 + \vec{P}_4$. In the relativistic limit ($s \gg 4m^2$), we find $s = (E_1 + E_2)^2 = 4E^2$ (with $E = E_1 = E_2$), $t = -\frac{s}{2}(1 - \cos\theta^*)$ and $u = -\frac{s}{2}(1 + \cos\theta^*)$.

Writing $\theta_{\mu\nu}$ as $c_{\mu\nu}/\Lambda_{NC}^2$ and taking all the nonvanishing $c_{\mu\nu}$ to be unity [10], we evaluate the quantities appearing in the squared-amplitude as

$$\begin{aligned} p_3\theta p_1 - p_4\theta p_2 &= \frac{s}{2\Lambda_{NC}^2} [1 - \cos\theta^* - \sin\theta^*(\cos\phi + \sin\phi)], \\ p_4\theta p_1 - p_3\theta p_2 &= \frac{s}{2\Lambda_{NC}^2} [1 + \cos\theta^* + \sin\theta^*(\cos\phi + \sin\phi)]. \end{aligned} \quad (\text{B3})$$

APPENDIX C: SQUARED AMPLITUDE OF THE BHABHA ($e^-(p_1)e^+(p_2) \rightarrow e^-(p_3)e^+(p_4)$) SCATTERING

Here we present several squared-amplitude terms of Eq.(13). We define p_1 , p_2 and p_3 , p_4 are the 4-momenta of the initial e^- and e^+ and the final e^- and e^+ . The terms in the squared matrix element are given by

$$\begin{aligned} \overline{|\mathcal{A}_{1B}^\gamma|^2} &= \frac{e^4}{4s^2} (1 + \frac{1}{4}E^2) Tr[\not{p}_2\gamma_\mu\not{p}_1\gamma_\nu] \times Tr[\not{p}_3\gamma^\mu\not{p}_4\gamma^\nu], \\ \overline{|\mathcal{A}_{2B}^\gamma|^2} &= \frac{e^4}{4t^2} (1 + \frac{1}{4}F^2) Tr[\not{p}_1\gamma_\nu\not{p}_3\gamma_\mu] \times Tr[\not{p}_4\gamma^\nu\not{p}_2\gamma^\mu], \\ \overline{|\mathcal{A}_{1B}^Z|^2} &= \frac{e^4}{4x_W^4(s - m_Z^2)^2} (1 + \frac{1}{4}E^2) Tr[\not{p}_1\gamma_\nu\Gamma_A^-\not{p}_2\gamma_\mu\Gamma_A^-] \times Tr[\not{p}_4\gamma^\nu\Gamma_A^-\not{p}_3\gamma^\mu\Gamma_A^-], \\ \overline{|\mathcal{A}_{2B}^Z|^2} &= \frac{e^4}{4x_W^4(t - m_Z^2)^2} (1 + \frac{1}{4}F^2) Tr[\not{p}_1\gamma_\nu\Gamma_A^-\not{p}_3\gamma_\mu\Gamma_A^-] \times Tr[\not{p}_4\gamma^\nu\Gamma_A^-\not{p}_2\gamma^\mu\Gamma_A^-], \\ -2\overline{Re(\mathcal{A}_{1B}^\gamma\mathcal{A}_{2B}^{\gamma*})} &= -\frac{e^4}{2st} Re \left[(1 + \frac{i}{2}E)(1 + \frac{i}{2}F) Tr[\not{p}_1\gamma_\nu\not{p}_3\gamma^\mu\not{p}_4\gamma^\nu\not{p}_2\gamma_\mu] \right], \\ +2\overline{Re(\mathcal{A}_{1B}^\gamma\mathcal{A}_{1B}^{Z*})} &= \frac{e^4}{2x_W^2s(t - m_Z^2)} Re \left[(1 + \frac{1}{4}E^2) Tr[\not{p}_1\gamma_\nu\Gamma_A^-\not{p}_2\gamma_\mu] Tr[\not{p}_4\gamma^\nu\Gamma_A^-\not{p}_3\gamma^\mu] \right], \\ -2\overline{Re(\mathcal{A}_{1B}^\gamma\mathcal{A}_{2B}^{Z*})} &= -\frac{e^4}{2x_W^2s(t - m_Z^2)} Re \left[(1 + \frac{i}{2}E)(1 + \frac{i}{2}F) Tr[\not{p}_1\gamma_\nu\Gamma_A^-\not{p}_3\gamma_\mu\not{p}_4\gamma^\nu\Gamma_A^-\not{p}_2\gamma^\mu] \right], \\ -2\overline{Re(\mathcal{A}_{2B}^\gamma\mathcal{A}_{1B}^{Z*})} &= -\frac{e^4}{2x_W^2t(s - m_Z^2)} Re \left[(1 - \frac{i}{2}E)(1 - \frac{i}{2}F) Tr[\not{p}_1\gamma_\nu\Gamma_A^-\not{p}_2\gamma^\mu\not{p}_4\gamma^\nu\Gamma_A^-\not{p}_3\gamma_\mu] \right], \\ +2\overline{Re(\mathcal{A}_{2B}^\gamma\mathcal{A}_{2B}^{Z*})} &= \frac{e^4}{2x_W^2u(u - m_Z^2)} Re \left[(1 + \frac{1}{4}F^2) Tr[\not{p}_1\gamma_\nu\Gamma_A^-\not{p}_4\gamma_\mu] Tr[\not{p}_2\gamma^\nu\Gamma_A^-\not{p}_3\gamma^\mu] \right], \\ -2\overline{Re(\mathcal{A}_{1B}^Z\mathcal{A}_{2B}^{Z*})} &= -\frac{e^4}{2x_W^4(u - m_Z^2)(t - m_Z^2)} Re \left[(1 + \frac{i}{2}E)(1 + \frac{i}{2}F) Tr[\not{p}_1\gamma_\nu\Gamma_A^-\not{p}_4\gamma_\mu\Gamma_A^-\not{p}_2\gamma^\nu\Gamma_A^-\not{p}_3\gamma_\mu\Gamma_A^-] \right], \end{aligned} \quad (\text{C1})$$

where $E = (p_2\theta p_1 + p_4\theta p_3)$, $F = (p_3\theta p_1 + p_4\theta p_2)$. In the c.o.m frame of $e^-(p_1) - e^+(p_2)$ collision, with the 4-momenta prescription as discussed above, we then evaluate the quantities

$$\begin{aligned} p_2\theta p_1 + p_4\theta p_3 &= \frac{s}{2\Lambda_{NC}^2} [1 + \cos\theta^* + \sin\theta^*(\cos\phi + \sin\phi)], \\ p_3\theta p_1 + p_4\theta p_2 &= \frac{s}{2\Lambda_{NC}^2} [\sin\theta^*(\cos\phi + \sin\phi)]. \end{aligned} \tag{C2}$$

-
- [1] H.S. Snyder, Phys. Rev. D **71**, 38 (1947).
- [2] A.Connes,M.R.Douglas and A.Schwarz, J. High Energy Physics **02**, 003 (1998).
- [3] M.R.Douglas and C.Hull, J. High Energy Physics **02**, 008 (1998).
- [4] N. Seiberg and E. Witten, J. High Energy Physics **09**, 032 (1999).
- [5] V. Schomerus, J. High Energy Physics **06**, 030 (1999).
- [6] B. Jurco, P. Schupp and J. Wess, Mod. Phys. Lett. **A16**, 343 (2001).
- [7] E.Witten, Nucl. Phys. **B471**, 135 (1996); P.Horava and E.Witten, Nucl. Phys. **B460**, 506 (1996).
- [8] M. R. Douglas and N. Nekrasov, Rev. Mod. Phys. **73**, 977 (2001); I. F. Riad and M. M. Sheikh-Jabbari, J. High Energy Physics **08**, 45 (2000); B. Jurco and P. Schupp, Eur. Phys. J. C **14**, 367 (2000).
- [9] X. Calmet, B. Jurco, P. Schupp, J. Wess and M. Wohlgenannt, Eur. Phys. J. C **23**, 363 (2002); X. Calmet Eur. Phys. J. C **50**, 113 (2007); X. Calmet and M. Wohlgenannt Phys. Rev. D **68**, 025016 (2003).
- [10] J.Hewett, F.J.Petriello and T.G.Rizzo, hep-ph/0201275; J.Hewett *et al.*, Phys. Rev. D **64**, 075012 (2001), Phys. Rev. D **66**, 036001 (2002); T. G. Rizzo Int. J. Mod. Phys. **A18**, 2797 (2003); I. Hinchliffe, N. Kersting and Y. L. Ma, Int. J. Mod. Phys. **A19**, 179 (2004); A. Alboteanu, T. Ohl and R. Ruckl, Acta Phys. Pol. B **38**, 3647 (2007).
- [11] B. Melić, K. P. Kumericki, J. Trampetic, P. Schupp and M. Wohlgenannt Eur. Phys. J. C **42**, 483 (2005); B. Melić *et al.*, Eur. Phys. J. C **42**, 499 (2005). P. Schupp and J. Trampetic, Springer Proc.Phys. **98**, 219 (2005); P. Schupp, Lect. Notes Phys. **616**, 305 (2003).
- [12] G. Duplancic, P. Schupp and J. Trampetic Eur. Phys. J. C **32**, 141 (2003); W. Behr, N. G. Deshpande, G. Duplancic, P. Schupp, J. Trampetic and J. Wess, Eur. Phys. J. C **29**, 441 (2003); P. Aschieri, B. Jurco, P. Schupp and J. Wess Nucl. Phys. **B651**, 45 (2003).